INTERNATIONAL JOURNAL OF ADAPTIVE CONTROL AND SIGNAL PROCESSING
Int. J. Adapt. Control Signal Process. 2004; **18**:245–263 (DOI: 10.1002/acs.792)

Blind MIMO equalization with optimum delay using independent component analysis

Vicente Zarzoso*,† and Asoke K. Nandi

Department of Electrical Engineering and Electronics, The University of Liverpool, Brownlow Hill, Liverpool L69 3GJ, U.K.

SUMMARY

Blind space–time equalization of multiuser time-dispersive digital communication channels consists of recovering the users' simultaneously transmitted data free from the interference caused by each other and the propagation effects, without using training sequences. In scenarios composed of mutually independent non-Gaussian i.i.d. users' signals, independent component analysis (ICA) techniques based on higher-order statistics can be employed to refine the performance of conventional linear detectors, as recently shown in a code division multiple access environment (*Signal Process* 2002; **82**:417–431). This paper extends these results to the more general multi-input multi-output (MIMO) channel model, with the minimum mean square error (MMSE) as conventional equalization criterion. The time diversity introduced by the wideband multipath channel enables a reduction of the computational complexity of the ICA post-processing stage while further improving performance. In addition, the ICA-based detector can be tuned to extract each user's signal at the delay which provides the best MMSE. Experiments in a variety of simulation conditions demonstrate the benefits of ICA-assisted MIMO equalization. Copyright © 2004 John Wiley & Sons, Ltd.

KEY WORDS: blind source separation; blind space–time equalization; equalization delay; higher-order statistics; independent component analysis; MIMO channel; MMSE detection; multiuser communications; SIMO channel; second-order statistics

1. INTRODUCTION

Blind space–time equalization—motivation. Future wireless communication systems are expected to support a wide variety of high data rate multimedia applications [1, 2]. Increased transmission speeds combined with multipath propagation environments result in highly time-dispersive (or frequency selective) channels, which introduce severe intersymbol interference (ISI) in the received signal [3]. Novel multiple access techniques are currently being investigated whereby simultaneous transmission of different users in the same time–frequency slot is allowed (e.g.

*Correspondence to: Vicente Zarzoso, Department of Electrical Engineering and Electronics, The University of Liverpool, Brownlow Hill, Liverpool L69 3GJ, U.K.
† E-mail: vicente@liv.ac.uk

Contract/grant sponsor: Royal Academy of Engineering, U.K.

Received 11 August 2003
Revised 13 October 2003
Accepted 17 October 2003

spatial division multiple access, SDMA). This overlapped sharing of channel resources enhances bandwidth utilization at the expense of an increased level of co-channel interference (CCI). Signal processing techniques for space–time equalization aim at the cancellation of CCI and ISI at the receive antenna output, and the recovery of the transmitted users' data [4]. Traditionally, equalization is aided with the transmission of training or pilot sequences, which makes a poor use of the available bandwidth and is not feasible or practical in certain scenarios [5, 6]; hence the enormous research interest aroused by blind equalization techniques since the seminal works of References [7–11].

SIMO model. In the single-user case, the use of receivers with spatially separated multiple antenna elements and/or oversampling (i.e. sampling faster than the baud rate) leads to the single-input multiple-output (SIMO) signal model. Compared to the conventional single-output (SISO) case, SIMO systems exhibit two remarkable features [12–14]: first, non-minimum phase channels can be blindly identified using only second-order statistics (SOS); second, finite impulse response (FIR) channels can be perfectly equalized, in the noiseless case, using FIR filters.

MIMO model—ICA-based CCI-cancellation. The multiuser scenario is naturally described by the multiple-input multiple-output (MIMO) signal model. This model also arises in systems with multiple transmitter antennas (using, e.g. spatial multiplexing), even if just a single user is present. The MIMO extensions of SIMO equalization techniques are able to suppress ISI, resulting in a memoryless CCI-only cancellation problem [5, 15–17]. This latter can then be resolved using source separation techniques based on the finite alphabet or constant modulus properties of digital modulations [5,18–20]. Alternatively, the mutual statistical independence between the users' signals can be exploited through the use of independent component analysis (ICA) [21] based on higher-order statistics (HOS) [15, 22–24]. The main advantage of HOS-based ICA techniques is that, under mild conditions (typically, that at most one of the sources be Gaussian [23]), signal recovery is guaranteed regardless of the source constellation and spectral characteristics [24].

Channel identification and optimum-delay estimation. Blind multichannel equalization can be performed with (e.g. References [12, 13, 25]) or without (e.g. References [5, 26, 27]) previous channel identification. Channel identification-based equalization presents the main drawback that inaccuracies in the channel estimate have a detrimental effect on the signal detection stage. However, a channel estimate may prove useful in a variety of tasks such as power control, propagation characterization, or source localization and tracking. More importantly, knowledge of the channel structure makes it possible to select the equalization delay which yields optimum performance. The equalized signal mean square error (MSE) for a given delay depends on the corresponding column of the channel matrix, as shown in the exact MSE expression for the linear minimum mean square error (MMSE) equalizer [28] as well as in the approximated Cramér–Rao lower bound of Reference [29]. Even direct equalization methods require to estimate the channel response from the equalized output in order to perform optimum delay selection [27, 30]. In addition, Reference [27] needs to compute the equalizers for all delays before discerning the optimum solution. The iterative procedure described in Reference [31] avoids channel estimation, but its convergence to the optimum-delay equalizer is only conjectured and is not theoretically guaranteed; the procedure is also computationally expensive.

ICA-based detection. The exploitation of HOS through ICA proves useful in refining conventional linear detection, as recently demonstrated in Reference [1] in a particular code division multiple access (CDMA) model. The ICA refinement alleviates the negative impact of

channel estimation errors on the equalization performance. Similar results are obtained in Reference [32] in the more generic MIMO model, where it is shown that ICA-aided MMSE equalization outperforms the conventional MMSE receiver. Furthermore, the time redundancies of the MIMO model allow certain simplifications which yield considerable performance improvements with significant computational savings.

Contribution. The purpose of this paper is to elaborate on the findings of Reference [32]. We propose the use of ICA for the simultaneous extraction of the users' signals at their respective optimal MMSE equalization delays. The subsequent performance gains are achieved at only a modest increase in computational load relative to the conventional receiver. We also intend to carry out, through simulation, a more rigorous experimental analysis of ICA-assisted blind detection in MIMO digital communication systems.

Outline of the paper. Section 2 summarizes the signal model and mathematical preliminaries. Section 3 presents the theory behind ICA-aided optimum-delay equalization, which is the core of our contribution. An experimental study is reported in Section 4. The concluding remarks of Section 5 bring the paper to an end.

Notations. Vectors and matrices are denoted by boldface lowercase and uppercase symbols, respectively; $\mathbb{C}$ is the set of complex numbers; $\mathbf{I}_n$ refers to the $n \times n$ identity matrix; $(\cdot)^{\mathrm{T}}$, $(\cdot)^{\mathrm{H}}$, $(\cdot)^{-1}$ and $(\cdot)^{\dagger}$ indicate the transpose, Hermitian (conjugate-transpose), inverse and Moore-Penrose pseudoinverse matrix operators, respectively; $(\mathbf{a})_i$ is ith component of vector $\mathbf{a}$; $\|\mathbf{A}\|_{\mathrm{F}}^2 = \mathrm{trace}(\mathbf{A}\mathbf{A}^{\mathrm{H}}) = \mathrm{trace}(\mathbf{A}^{\mathrm{H}}\mathbf{A})$ denotes the Frobenius norm of matrix $\mathbf{A}$; $\mathbb{R}\mathrm{e}(\cdot)$ denotes the real part of its complex argument; $\mathrm{E}\{\cdot\}$ represents the mathematical expectation; $\otimes$ and $\odot$ stand for the Kronecker and elementwise product, respectively.

2. SIGNAL MODEL

Let us consider a multiuser communication system composed of

(A1) K users transmitting, at a known constant baud rate, zero-mean unit-variance mutually independent non-Gaussian i.i.d. data symbols $\mathbf{s}(n) = [s_1(n), \ldots, s_K(n)]^{\mathrm{T}} \in \mathbb{C}^K$,
(A2) a receiver with vector output $\mathbf{x}(n) = [x_1(n), \ldots, x_L(n)]^{\mathrm{T}} \in \mathbb{C}^L$,
(A3) FIR channels (including pulse-shaping and receive filter effects) spanning at most $M+1$ symbols, with matrix coefficients $\mathbf{H}(k) \in \mathbb{C}^{L\times K}$, $k = 0, 1, \ldots, M$, where the channel order M is assumed to be known and the channel taps fixed over the observation window,
(A4) zero-mean additive noise $\mathbf{v}(n) \in \mathbb{C}^L$ independent of the data sources.

Symbols n and k above represent discrete-time indices relative to the baud period. The receiver output components in (A2) are not necessarily associated with spatially separated physical devices. Since digital signals are cyclostationary, oversampling or fractionally spaced sampling (i.e. taking more than a sample per baud period) can induce extra 'virtual' sensors [12, 13]. The virtual channels are given by the phases of the physical channels, a phase corresponding to a baud-sampled sequence of the impulse response with a different time origin. Space–time processing operates on the spatial (physically separated sensors) as well as the temporal dimension [4, 5]. Although time- or space-only processing may suffice in theory, improved ISI-CCI suppression can be achieved by joint space–time processing [4]. Assumptions (A3) model block (or time-non-selective or slowly) fading channels, typical of low mobility systems, with small to moderate Doppler spread values.

Under the above assumptions, the MIMO model can be expressed as

$$\mathbf{x}(n) = \sum_{k=0}^{M} \mathbf{H}(k)\mathbf{s}(n-k) + \mathbf{v}(n) \tag{1}$$

Stacking N consecutive received signal vector samples leads to the matrix model

$$\mathbf{x}_n = \mathbf{H}\mathbf{s}_n + \mathbf{v}_n \tag{2}$$

with $\mathbf{s}_n = [\mathbf{s}(n)^{\mathrm{T}}, \mathbf{s}(n-1)^{\mathrm{T}}, \ldots, \mathbf{s}(n-M-N+1)^{\mathrm{T}}]^{\mathrm{T}} \in \mathbb{C}^{K(M+N)}$

$$\mathbf{H} = \begin{bmatrix} \mathbf{H}(0) & \cdots & \mathbf{H}(M) & 0 & \cdots & 0 \\ 0 & \mathbf{H}(0) & \cdots & \mathbf{H}(M) & \cdots & 0 \\ \vdots & \ddots & \ddots & \ddots & \ddots & \vdots \\ 0 & \ldots & 0 & \mathbf{H}(0) & \cdots & \mathbf{H}(M) \end{bmatrix} \tag{3}$$

$\mathbf{x}_n = [\mathbf{x}(n)^{\mathrm{T}}, \mathbf{x}(n-1)^{\mathrm{T}}, \ldots, \mathbf{x}(n-N+1)^{\mathrm{T}}]^{\mathrm{T}} \in \mathbb{C}^{LN}$, and analogous definition for $\mathbf{v}_n$. For convenience, we call $P = LN$, $C = M + N$, and $D = KC$.

The objective of blind MIMO equalization is to estimate the source signals $\mathbf{s}(n)$ from the only observation of the receiving sensor output $\mathbf{x}(n)$. This process involves ISI cancellation (time equalization) and CCI suppression (space equalization). These tasks can be performed by first identifying the channel taps

$$\underline{\mathbf{H}} = [\mathbf{H}(0), \mathbf{H}(1), \ldots, \mathbf{H}(M)] \tag{4}$$

which are then 'inverted' to estimate the sources. The block-Toeplitz channel matrix $\mathbf{H} \in \mathbb{C}^{P \times D}$ in Equation (2) must be full column rank. An obvious necessary condition is that $L > K$: the number of sensors must be strictly higher than the number of sources, i.e. sufficient spatio-temporal diversity must be available; also, $N \geqslant KM/(L-K)$, which sets a lower bound on the equalizer length. A sufficient condition for the invertibility of $\mathbf{H}$ is that the subchannels be coprime, that is, that they do not share any common zeros [12]. More elaborate sufficient conditions are given in Reference [33].

Even if the channel matrix is invertible, inherent indeterminacies exist. Without any further prior knowledge on the sources or the mixing system besides assumptions (A1) and (A3), the channel matrix taps $\mathbf{H}(k)$ can at best be identified up to a common post-multiplicative factor $\mathbf{\Lambda\Gamma}$, where $\mathbf{\Gamma} \in \mathbb{C}^{K \times K}$ is a permutation matrix and $\mathbf{\Lambda} \in \mathbb{C}^{K \times K}$ a non-singular diagonal matrix with unit-norm diagonal elements. These phase and permutation indeterminacies are unavoidable but admissible ambiguities in blind estimation.

In the sequel, it is assumed that the channel matrix $\mathbf{H}$ (or, equivalently, the channel tap matrix $\underline{\mathbf{H}}$) has been estimated through a suitable blind MIMO identification method (as those of, e.g. References [5, 16, 17, 32]). Our primary concern is the estimation (i.e. detection or equalization) of the source signals $\mathbf{s}$ from the sensor output $\mathbf{x}$ by using the identified channel. In blind space–time equalization techniques based on previous channel identification, ISI-CCI suppression is implicitly carried out during channel estimation, and actually takes effect at the detection stage.

3. ICA-AIDED DETECTION

3.1. Linear detection

Even if the channel is perfectly known, the estimation of the source signals in a noisy model like (1)–(2) is not a trivial task. The maximum likelihood sequence estimator is the optimal detector, but its computational load can be prohibitive in scenarios involving a large number of users and highly dispersive channels [3]. Trading off complexity for performance, linear receivers are based on the estimation of a linear transformation $\mathbf{G} \in \mathbb{C}^{P \times D}$ fulfilling certain (sub)optimality criterion; data are then detected as $\hat{\mathbf{s}}_n = \mathbf{G}^{\mathrm{H}}\mathbf{x}_n$. The zero forcing (ZF) detector aims at the joint minimization of ISI and CCI in the absence of noise, and can thus be expressed as the least-squares problem

$$\mathbf{G}_{\mathrm{ZF}} = \arg \min_{\mathbf{G}} \|\mathbf{G}^{\mathrm{H}}\mathbf{H} - \mathbf{I}_D\|_{\mathrm{F}}^2 \tag{5}$$

The solution to (5) is readily computed as $\mathbf{G}_{\mathrm{ZF}} = (\mathbf{H}\mathbf{H}^{\mathrm{H}})^{-1}\mathbf{H} = (\mathbf{H}^{\dagger})^{\mathrm{H}}$. The ZF detector can lead to severe noise amplification in noisy scenarios. This drawback is avoided by the minimum mean square error (MMSE) equalizer

$$\mathbf{G}_{\mathrm{MMSE}} = \arg \min_{\mathbf{G}} \mathrm{E}\{\|\mathbf{G}^{\mathrm{H}}\mathbf{x}_n - \mathbf{s}_n\|^2\} \tag{6}$$

with closed-form solution $\mathbf{G}_{\mathrm{MMSE}} = \mathbf{R}_x^{-1}\mathbf{H}$, where $\mathbf{R}_x = \mathrm{E}\{\mathbf{x}\mathbf{x}^{\mathrm{H}}\}$ represents the sensor-output covariance matrix. Due to its enhanced properties at low signal-to-noise ratio (SNR), we adhere to the MMSE detector in the following. The development is analogous for ZF equalization.

3.2. ICA refinement

Imprecisions, e.g. due to finite sample size, in the estimation of the channel matrix or the sensor covariance matrix have a negative impact on the detection of the transmitted data symbols. To alleviate this detrimental effect, the higher-order statistical independence of the users' signals can be exploited. Under the spatio-temporal independence assumption of (A1), model (2) corresponds to a problem of blind separation of independent sources in instantaneous linear mixtures, which can be solved with the statistical tool of ICA based on HOS [21]. From this perspective, the source estimation can be carried out without previous channel identification by applying an ICA method directly and then using a simple algorithm to identify and group each user's delays [24, 34, 35]. Although this fully blind ICA approach is conceptually simple, the computational complexity of separating $D = K(M + N)$ independent components can become excessive, even with a moderate number of users, in systems with long delay spreads as a result of high data rates [24].

The rationale behind ICA-assisted detection consists of taking advantage of the available channel estimate as an initial point in the ICA search. Two main benefits can be derived from this refinement. Firstly, since conventional detection (Equations (5)–(6)) only makes use (implicitly) of SOS, the exploitation of HOS by ICA is expected to mitigate performance drops caused by estimation errors at the channel identification stage. Secondly, if these channel identification errors are moderate, the initialization provided by the channel estimate may already be quite close to the ICA solution, thus decreasing the convergence time and computational complexity of the ICA post-processing block. The idea of ICA-refined detection was originally proposed in Reference [1] in the context of a DS-CDMA signal model. In

Reference [32], the ICA-based MMSE refinement was extended to the more general MIMO model, and is reproduced below for the sake of completeness.

Consider the whitened sensor output $\mathbf{z}_n = \mathbf{W}\mathbf{x}_n$, in which the whitening matrix $\mathbf{W} \in \mathbb{C}^{D\times P}$ constrains $\mathbf{R}_z = \mathbf{I}_D$. Matrix $\mathbf{W}$ can easily be computed from the eigenvalue decomposition (EVD) of $\mathbf{R}_x$, and involves second-order space–time decorrelation, power normalization and projection on the signal subspace. The MMSE estimate of $\mathbf{s}_n$ accepts the equivalent expression $\hat{\mathbf{s}}_n = \tilde{\mathbf{G}}^{\mathrm{H}}\mathbf{z}_n$, with

$$\tilde{\mathbf{G}} = \mathbf{W}\hat{\mathbf{H}} \tag{7}$$

In the noiseless case, detection matrix $\tilde{\mathbf{G}}$ is unitary. Hence, the whitened outputs can be regarded as a spatio-temporal unitary linear mixture of the users' data. To exploit the source statistical independence, an ICA method can operate on the whitened signals $\mathbf{z}_n$ with a separating matrix initialized at the conventional MMSE detection matrix $\tilde{\mathbf{G}}$. Final detection is then performed with the separating matrix $\hat{\mathbf{G}}$ provided by the ICA algorithm at convergence. The use of HOS constrains the users' data to be non-Gaussian (Assumption (A1)), which is verified by most digital modulations of practical significance. We select the fixed-point FastICA algorithm based on kurtosis optimization [21, 36] for its robustness and rapid (cubic) convergence properties. Assume that T consecutive whitened column vectors are stored in matrix $\mathbf{Z} = [\mathbf{z}_0, \mathbf{z}_1, \ldots, \mathbf{z}_{T-1}] \in \mathbb{C}^{D\times T}$. The FastICA algorithm can be outlined as follows [1, 21, 36]:

1. Initialize $\hat{\mathbf{G}}_0$ as the projection of $\tilde{\mathbf{G}}$ onto the set of unitary matrices.
2. For $k \geqslant 0$, repeat steps below until convergence.
3. $\hat{\mathbf{S}}_k = \hat{\mathbf{G}}_k^{\mathrm{H}}\mathbf{Z}$.
4. Update $\hat{\mathbf{G}}_{k+1} = \frac{1}{T}\mathbf{Z}(|\hat{\mathbf{S}}_k|^2 \odot \hat{\mathbf{S}}_k)^{\mathrm{H}} - \gamma\hat{\mathbf{G}}_k$.
5. Symmetric decorrelation $\hat{\mathbf{G}}_{k+1} \leftarrow \hat{\mathbf{G}}_{k+1}(\hat{\mathbf{G}}_{k+1}^{\mathrm{H}}\hat{\mathbf{G}}_{k+1})^{-1/2}$.

In Step 4, $\gamma = 3$ for real-valued sources (e.g. BPSK modulations) and $\gamma = 2$ for complex-valued sources. The orthogonal projection on the set of unitary matrices of Steps 1 and 5 admits an efficient implementation in terms of the singular value decomposition (SVD) $\hat{\mathbf{G}} = \mathbf{U}\boldsymbol{\Sigma}\mathbf{V}^{\mathrm{H}}$ as $\hat{\mathbf{G}} \leftarrow \mathbf{U}\mathbf{V}^{\mathrm{H}}$. As a statistically significant termination criterion we choose

$$\left|\frac{1}{D}\mathrm{trace}(|\hat{\mathbf{G}}_{k+1}^{\mathrm{H}}\hat{\mathbf{G}}_k|) - 1\right| < \frac{10^{-3}}{T} \tag{8}$$

That is, iterations are stopped when the column vectors of $\hat{\mathbf{G}}_{k+1}$ and $\hat{\mathbf{G}}_k$ lie in directions which are sufficiently close (in terms of a sample-size based threshold). In preliminary experiments, less than $2D$ iterations are typically required for convergence in high SNR environments and sufficient sample size. For low SNR or insufficient sample length, the algorithm may not converge, so the above maximum number of iterations is set as an additional termination test. Excluding the symmetric decorrelation step, the computational complexity of the FastICA algorithm is of order $O(DT)$ floating point operations (flops) per column of $\hat{\mathbf{G}}$ per iteration.

Note that the authors of Reference [1] were involved in extracting the signal of a single user of interest, whereas we aim at the simultaneous demodulation of all existing users (including all the spatially multiplexed data substreams of each user, if multiple transmit antennas are employed). Furthermore, the parameterization in the CDMA model of Reference [1] only accounts for channels with short delay spreads (more precisely, a delay spread of less than half the symbol period is considered in that reference). By contrast, the more general MIMO model of Equations (1)–(2) enables a more realistic characterization of wideband channels with longer

delay spreads.[‡] More importantly, Reference [1] extracts the user-of-interest's signal at a fixed delay. However, long delay spreads make it possible to extract the users' data at alternative delays, which can lead to potential performance improvements. Unlike fully blind ICA, where no control over the extracted delay is possible, we will see next that ICA-based MIMO equalization can be fine-tuned to carry out detection at the best delay for each user, thus improving performance while reducing computational cost.

3.3. Optimal delay selection

The previous sections have reviewed linear detectors that estimate all the components of the source vector $\mathbf{s}_n$ simultaneously, and how this conventional detection can be enhanced with the use of ICA. However, most of the detected signals are redundant, since $C = M + N$ time-shifted versions of each of the K users are recovered, whereas a single time delay suffices in practice. The time redundancy introduced by the multipath channel in the MIMO model (2) enables the choice of the equalization delay providing the best MMSE performance for each user. This choice is simplified thanks to the channel matrix estimate obtained in the blind identification stage.

The MMSE detector of the ith source signal, $1 \leqslant i \leqslant K$, with delay $0 \leqslant d \leqslant (C-1)$, is given by the corresponding column of $\mathbf{G}_{\mathrm{MMSE}}$:

$$\mathbf{G}_{i,d} = \mathbf{R}_x^{-1}\mathbf{h}_{i,d} \tag{9}$$

in which $\mathbf{h}_{i,d}$ denotes the $(Kd + i)$th column vector of channel matrix $\mathbf{H}$. The resulting MMSE can be obtained analytically as [28]

$$\mathrm{MMSE}_{i,d} = \mathrm{E}\{|\hat{s}_i(n-d) - s_i(n-d)|^2\} = 1 - \mathbf{h}_{i,d}^{\mathrm{H}}\mathbf{R}_x^{-1}\mathbf{h}_{i,d} \tag{10}$$

Optimum MMSE equalization for the ith user is achieved at delay

$$d_i = \arg\min_d \mathrm{MMSE}_{i,d} \tag{11}$$

Hence, from the available estimate of the channel matrix and the sensor output covariance matrix, it is possible to compute the equalizer that will detect each source signal with the lowest MMSE.

In practice, estimation errors caused by finite sample length may produce negative values of MMSE in Equation (10). However, in our experience the shape of the MMSE performance variation as a function of the equalization delay as well as the position of the optimum delay do not suffer significant changes relative to the theoretical solution.

3.4. Simplified ICA refinement

Once the optimal delay of each source has been selected, the corresponding columns of the estimated channel can be used to initalize the ICA post-processing stage. Let those columns be stored in matrix $\hat{\mathbf{H}}_K = [\mathbf{h}_{1,d_1}, \mathbf{h}_{2,d_2}, \ldots, \mathbf{h}_{K,d_K}]$. Then

$$\tilde{\mathbf{G}}_K = \mathbf{W}\hat{\mathbf{H}}_K \tag{12}$$

[‡] More details about the differences and relationships between channel models based on physical multipath parameters and on the channel impulse response can be found in Reference [4].

is the associated MMSE detector, which can serve as starting point for the ICA refinement (with the obvious modification of K for D in termination test (8)). In this manner, the ICA algorithm searches only for the K independent components associated with the users' signals at their respective optimum MMSE delay. This search for the optimum-delay components not only improves performance, but also leads to a reduction in computational complexity by a factor of C per iteration, which can be remarkable in highly time dispersive channels. In addition, since fewer independent components are sought, the ICA algorithm would also be expected to take fewer iterations to converge. These benefits will be put to the test in the experiments of Section 4.

This simplified MMSE-ICA detection scheme, which arises from the time redundancy induced by wideband multipath propagation, was originally proposed in Reference [32] for zero-delay equalization only. Herein, we improve on the original definition by allowing arbitrary delays and, in particular, those providing optimum MMSE performance for each user transmission.

3.5. Switching

The ICA refinement may converge to a solution far from optimal, worsening rather than improving the results of the conventional detector. Experimental results indicate that this undesirable outcome only occurs in low SNR scenarios or when processing short sample sizes. At low SNR, noise becomes dominant relative to the users' data in signal model (1)–(2). As a result, ICA will 'perceive' the noise as the actual sources, and thus will seek independence among the noise components. This misguided search will most probably yield a wrong equalization solution. Erroneous HOS estimation due to short observation windows can cause analogous adverse effects in the ICA refinement.

To avoid this degeneracy, a 'branch switching' criterion can be proposed along the lines of Reference [1]. By virtue of this criterion, the MMSE-ICA solution is deemed as favourable when the prior information provided by the conventional receiver is fairly preserved at the output of the ICA stage, that is, when the initial and final separating vectors (the columns of $\hat{\mathbf{G}}_0$ and $\hat{\mathbf{G}}$, respectively) are sufficiently correlated. This criterion can easily be extended to the MIMO model by switching to the MMSE-ICA solution of Section 3.2 whenever [32]

$$\xi \triangleq \frac{1}{D}\,\mathbb{R}\mathrm{e}(\mathrm{trace}(\hat{\mathbf{G}}^{\mathrm{H}}\hat{\mathbf{G}}_0)) > \tau \tag{13}$$

where $\tau \in]0,1[$ is a suitably selected threshold (e.g. Reference [1] chooses $\tau = 0.8$); the conventional MMSE detector is otherwise employed. Using K instead of D in the above expression, the switching rule is readily made applicable to the simplified MMSE-ICA solution of Section 3.4.

The usefulness of this switching strategy is arguable if the accuracy of the prior information acquired before detection (e.g. the proximity between the true and the identified channel) is poor. In such an event, the proposed switching could wrongly rule out ICA solutions that are actually advantageous compared to those of the linear MMSE receiver, which would be operating on erroneous information. This switching rule is tested in the simulations of next section.

4. EXPERIMENTAL RESULTS AND ANALYSIS

This section evaluates the comparative performance of the ICA-assisted equalizers under a variety of simulation conditions, and illustrates some points of the previous theoretical exposition. A communication system composed of $K = 5$ simultaneous QPSK-modulated users is simulated in a frequency-selective block fading channel introducing ISI from a maximum of $M = 4$ consecutive baud periods. The channel filter taps are randomly drawn from a complex Gaussian distribution and hence model (up to the pulse-shaping and receive filters) a Rayleigh propagation environment. A spatio-temporal oversampling level of $L = 10$ and a smoothing factor of $N = 5$ result in a 50×45 channel matrix $\mathbf{H}$. Additive white Gaussian noise with covariance matrix $\mathbf{R}_v = \sigma^2 \mathbf{I}_L$ is present at the sensor output; the SNR is given by

$$\mathrm{SNR} = \frac{\mathrm{trace}(\underline{\mathbf{H}}\,\underline{\mathbf{H}}^{\mathrm{H}})}{\sigma^2 L} \tag{14}$$

Equalization performance is measured by the signal mean square error (SMSE)

$$\mathrm{SMSE} = \frac{1}{K} \sum_{i=1}^{K} \mathrm{E}\{|\hat{s}_i(n - \hat{d}_i) - s_i(n - \hat{d}_i)|^2\} \tag{15}$$

where $\hat{d}_i$ represents the equalization delay selected for the ith user, which is obtained by the optimality criteria of Section 3.3 from the channel and covariance matrix estimates. Similarly, the channel identification accuracy can be assessed with the channel normalized mean square error (CMSE)

$$\mathrm{CMSE} = \frac{\|\underline{\hat{\mathbf{H}}} - \underline{\mathbf{H}}\|_{\mathrm{F}}^2}{\|\underline{\mathbf{H}}\|_{\mathrm{F}}^2} \tag{16}$$

where $\underline{\hat{\mathbf{H}}}$ is the estimated channel tap matrix. Performance parameters are averaged over v independent Monte Carlo (MC) iterations, with $vN_d \geqslant 10^5$, where N_d is the observation length in baud periods. As a quality index for the optimum-delay estimation performance we define the delay root mean square error (DRMSE)

$$\mathrm{DRMSE} = \sqrt{\frac{1}{v} \sum_{j=1}^{v} \frac{1}{K} \sum_{i=1}^{K} (\hat{d}_i^{(j)} - d_i)^2} \tag{17}$$

where $\hat{d}_i^{(j)}$ represents the ith-source delay estimate at MC iteration j, and theoretical values d_i are obtained from Equation (11) by plugging the true channel and covariance matrices in Equation (10).

4.1. Perfect channel knowledge

We first consider the scenario where the channel is assumed to be perfectly known or estimated, i.e. CMSE = 0. As a result, all errors in the MMSE equalizer are due exclusively to the finite-sample estimation of the sensor covariance matrix (or, equivalently in this case, of the noise variance), which is computed from N_d observed symbol periods. For instance, this scenario could simulate a training-based channel estimation preamble during transmission.

Performance vs sample size. Figure 1 shows the performance of the conventional MMSE, the MMSE-ICA and the simplified MMSE-ICA receivers against the sample size N_d, for SNR = 20 dB and a fixed channel matrix with condition number around 100. The ICA post-processing has difficulties to converge at low sample size, as shown by the number of FastICA iterations in Figure 2. A performance degradation is consequently observed when the switching criterion of

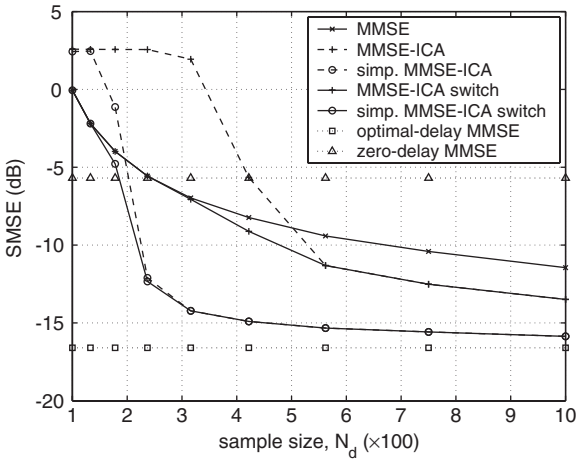

Figure 1. Equalization performance vs sample size, with CMSE = 0, SNR = 20 dB.

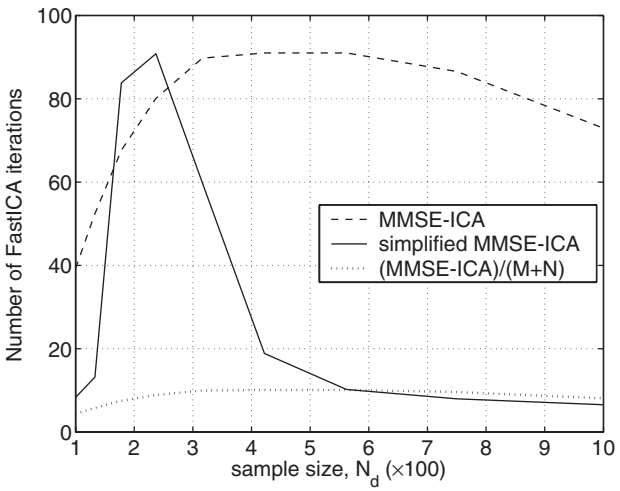

Figure 2. Number of FastICA iterations vs sample size in the simulation of Figure 1.

Section 3.5 is not implemented. However, as N_d gets sufficiently high the ICA receivers outperform the conventional equalizer, with the simplified MMSE-ICA obtaining the most efficient performance and approaching faster the theoretical lower bound. The iteration count of the latter then falls below $1/C$ times that of the full MMSE-ICA (Figure 2). According to Section 3.2, this means a reduction in flops by a factor of C^2.

Equalization delay. Figure 1 also compares the theoretical MMSE for the optimal- and the zero-delay equalizers, which emphasizes the gain that can be achieved by using the former. Illustrating this gain as well, Figure 3 plots the MMSE against the equalization delay for each source. The estimated optimum delay appears consistent and asymptotically unbiased, as shown in Figure 4. However, to keep the delay estimation accuracy more samples are needed as the SNR increases.

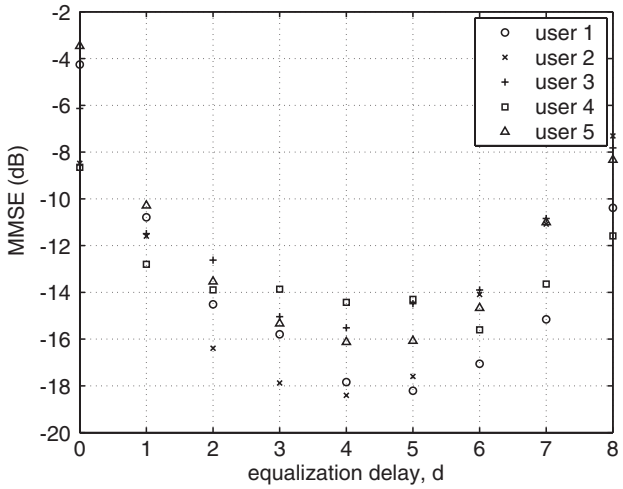

Figure 3. Theoretical MMSE performance vs equalization delay in the simulation conditions of Figure 1.

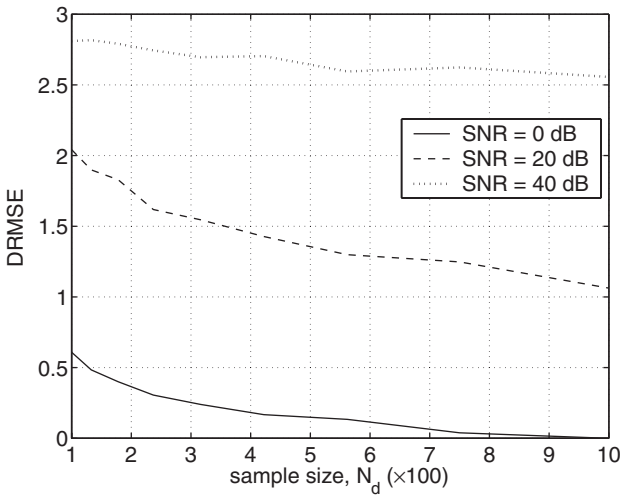

Figure 4. Optimum-delay estimation performance in the experiment of Figure 1, for several SNRs.

Switching threshold. In a bid to shed some light on the choice of the switching threshold τ, Figure 5 displays the loci of the average performance gain introduced by the ICA-aided detectors relative to the conventional MMSE, and their respective average correlation coefficient ξ, for various SNRs (0 , 20, 40, 60 dB, ∞). The plots indicate that $\tau \approx 0.8$ and $\tau \approx 0.6$ are good threshold choices for the MMSE-ICA and the simplified MMSE-ICA equalizer, respectively. In practice, the exact figures do not seem too critical. The 'switch' curves of Figure 1 were obtained with $\tau = 0.8$ for both ICA detectors, and such value has provided satisfactory results in all our experiments in a variety of different scenarios.

Performance vs SNR. The sensor covariance matrix estimation errors due to finite sample size cause interference flooring in the MMSE detector performance at high SNR, as soon as the

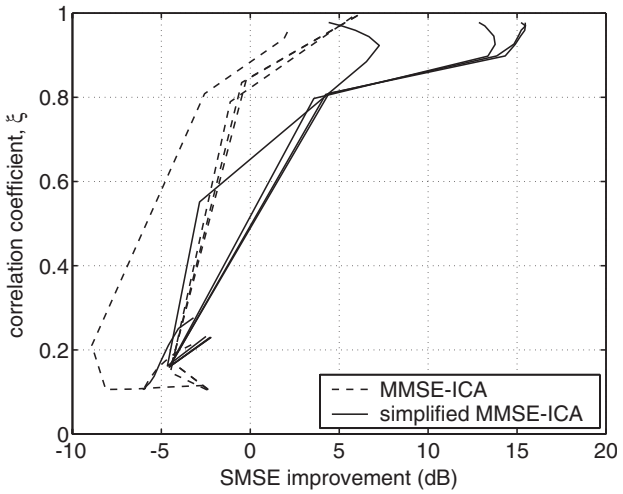

Figure 5. ICA performance gain vs correlation coefficient ξ for the scenario of Figure 1 and different SNRs.

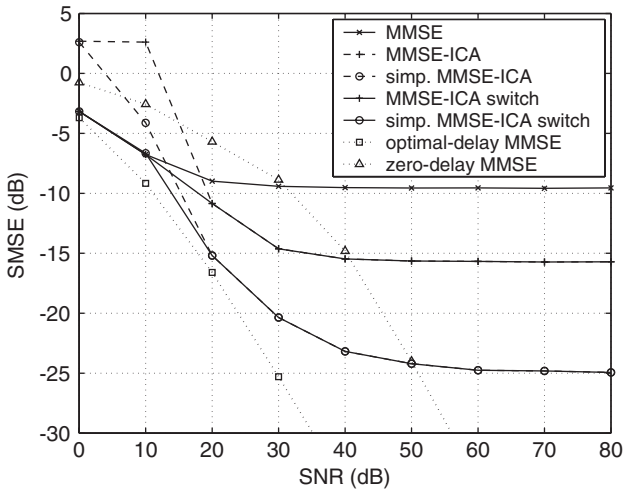

Figure 6. Equalization performance vs SNR, with CMSE $= 0$, $N_d = 500$.

sampling error overcomes the additive noise present at the sensor output. The success of ICA-based post-detection in tackling this adverse phenomenon is illustrated in Figure 6, which shows the performance of the different equalization schemes against the additive noise power, with an observation window of $N_d = 500$ baud periods and the same general conditions as above. MMSE-ICA alleviates the MMSE performance flooring by about 6 dB, whereas the simplified MMSE-ICA receiver provides a striking improvement of over 15 dB. Equivalently, the ICA detectors require about 3 and 12 times less samples, respectively, than the MMSE to achieve the same performance at high SNR.

Figure 7 shows that in low noise the MMSE-ICA actually converges in less iterations than the simplified MMSE-ICA. Hence, the ratio of C between both iteration counts seems to occur at moderate SNR levels only. On the other hand, Figure 8 illustrates again that more samples are needed to maintain the optimum-delay estimation quality as the SNR increases. This outcome, also observed in Figure 4, is closely related to the flooring effect commented above.

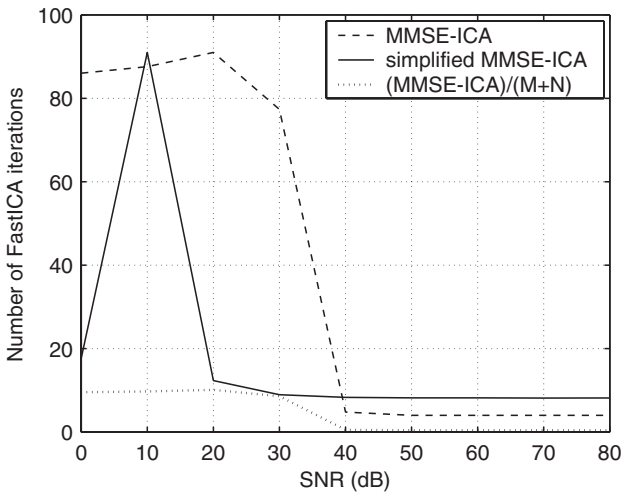

Figure 7. Number of FastICA iterations vs SNR in the experiment of Figure 6.

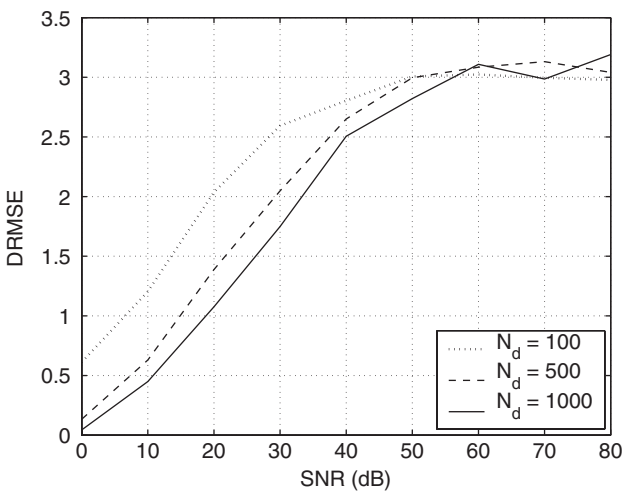

Figure 8. Optimum-delay estimation performance for the simulation conditions of Figure 6 and various sample lengths.

4.2. *Blindly identified channel*

In the experiments that follow, the channel is estimated from the sensor data using a suitable blind MIMO identification method. We choose the extension of the SIMO algorithm of Reference [12] followed by an ICA-based CCI-cancellation step, as explained in References [16, 24]. System parameters such as the channel order and the signal-subspace dimension are assumed as known.

Performance vs sample size. Figure 9 shows the detectors' performance as a function of the observed window size, when the sensor output SNR is 30 dB. The ICA-assisted equalizers

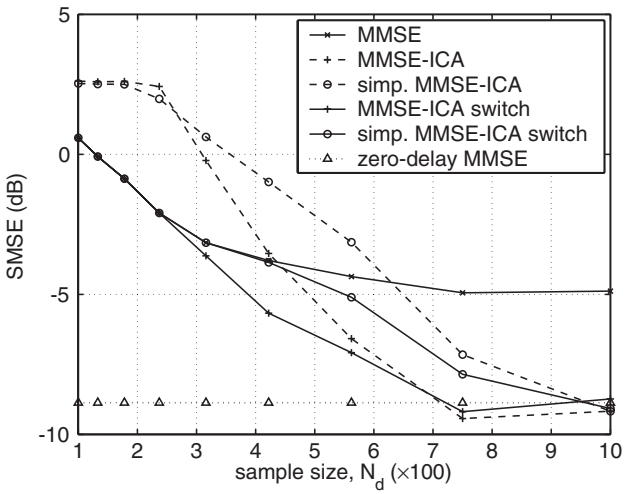

Figure 9. Blind equalization performance vs sample size, SNR = 30 dB.

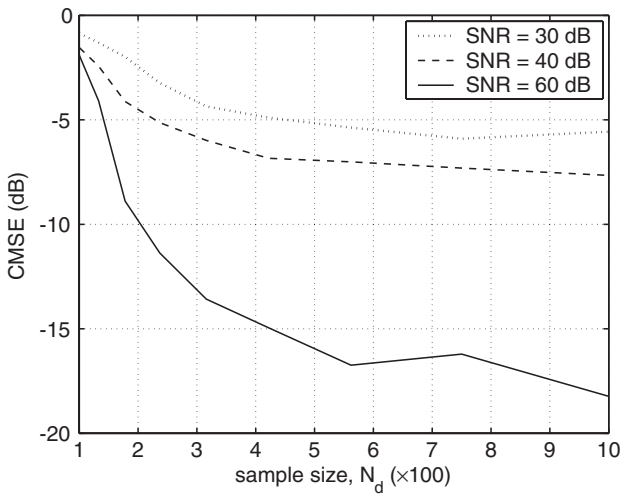

Figure 10. Blind channel identification performance for the simulation conditions of Figure 9 and several SNRs.

require around 500 samples to improve the conventional detector. This minimum sample length reduces for higher SNR (results for the noiseless case under similar simulation conditions can be found in Reference [32]). The theoretical optimal-delay MMSE lies around -25 dB, which the ICA methods are unable to reach due to an erroneous delay estimation (dashed line of Figure 11). Channel identification errors now join covariance matrix imprecisions in hindering an accurate delay detection. Indeed, the CMSE reaches only around -6 dB from about 700 samples in this simulation (dotted line in Figure 10). Despite the higher iteration count shown by the simplified MMSE-ICA in Figure 12, further experiments demonstrate that for high N_d and SNR both methods require approximately the same number of FastICA iterations.

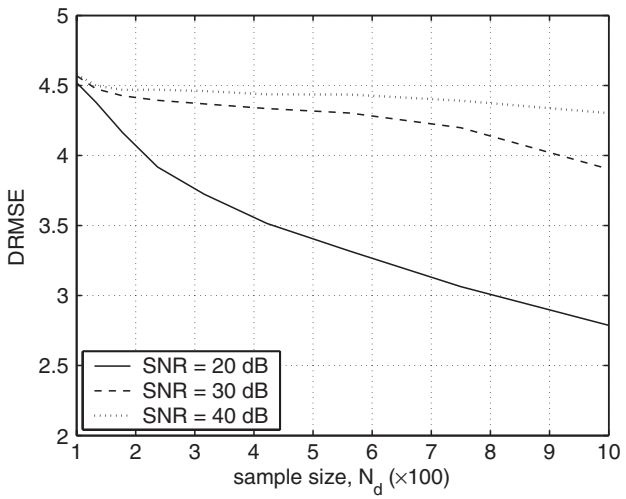

Figure 11. Delay estimation performance for the simulation conditions of Figure 9 and different SNRs.

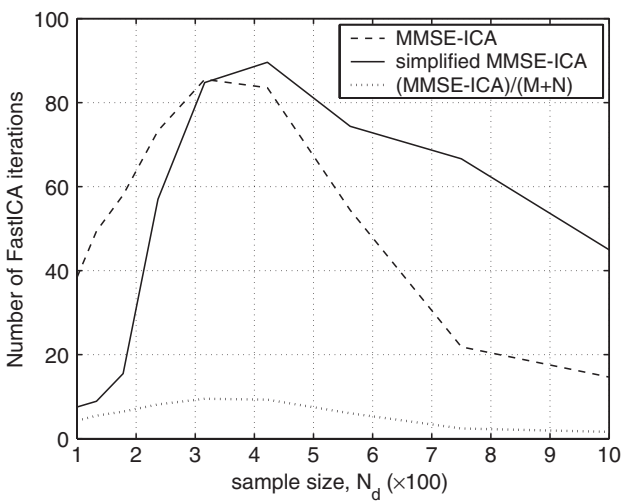

Figure 12. Number of FastICA iterations vs sample size in the simulation of Figure 9.

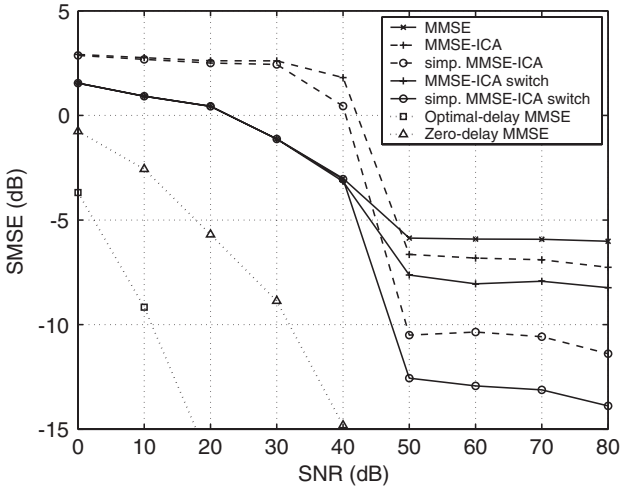

Figure 13. Blind equalization performance vs SNR, $N_d = 200$.

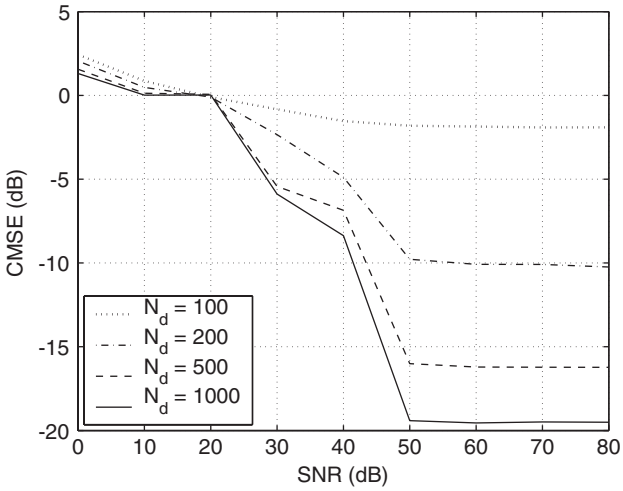

Figure 14. Blind channel identification performance for the simulation conditions of Figure 13 and various sample lengths.

Performance vs SNR. Figure 13 indicates that the ICA receivers outperform the MMSE detector with as few as $N_d = 200$ observed symbol periods, for a sensor output SNR above 40 dB. The benefits of the switching scheme can also be observed above that SNR value. The obtained CMSE at several sample lengths is shown in Figure 14. Delay estimation only accurate for sufficient window sizes at low SNR (Figure 15), as anticipated in the experiments with perfect channel knowledge. FastICA iteration counts for this simulation are displayed in Figure 16. The simplified MMSE-ICA method requires fewer iterations than the MMSE-ICA over

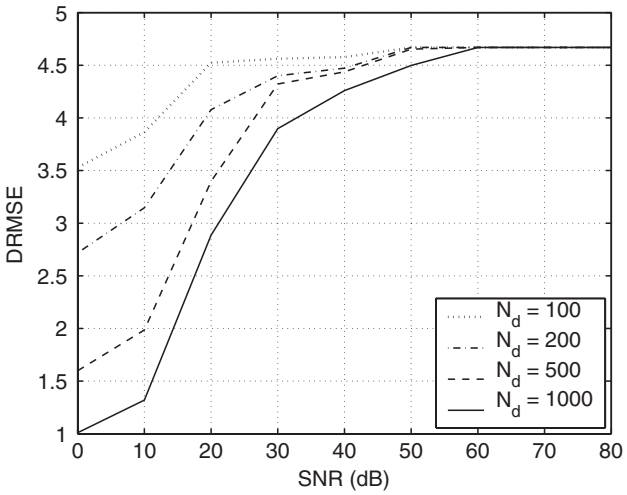

Figure 15. Delay estimation performance for the simulation conditions of Figure 13 and several sample lengths.

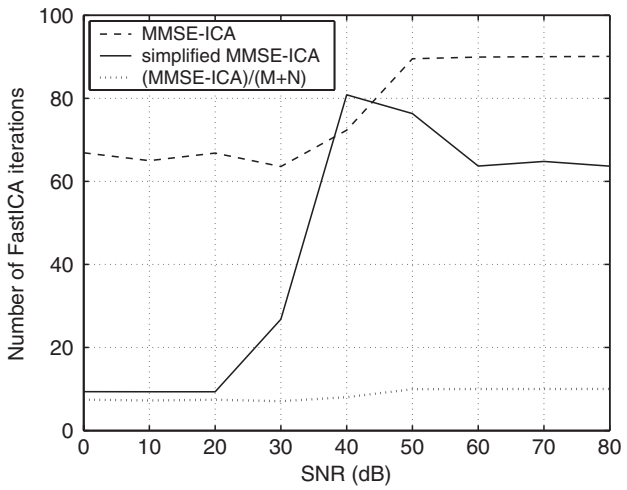

Figure 16. Number of FastICA iterations vs SNR for the simulation of Figure 13.

most of the SNR range, approaching the C factor at low SNR. In terms of flops, the simplified MMSE-ICA has proven less costly than the MMSE-ICA equalizer in all our experiments.

5. CONCLUSIONS

The users' statistical-independence, non-Gaussian, i.i.d. assumptions can be exploited to refine blind MIMO linear equalization through the use of ICA techniques based on HOS. The time diversity introduced by the wideband multipath channel leads to a simplification of the ICA-

assisted MMSE detector with improved performance and lower computational cost, by searching only for the equalization delays providing optimum MMSE for each user. The extension of these results to the SIMO model is straightforward.

It has been observed that a satisfactory optimum-delay detection depends on an accurate channel and sensor covariance matrix estimation, as well as a trade-off between SNR and observation length, whereby the required sample size increases as the noise power decreases. Nevertheless, even in situations where the channel and the delay estimates were rather inaccurate, the ICA-assisted detectors have been able to improve in all cases the conventional MMSE equalizer in moderate to high SNR and sample-size conditions. These conditions (e.g. just a few hundreds of observed baud periods) can be considered as realistic in practical scenarios.

Further work will consider the improvement of the optimum-equalization delay estimation, and will compare the ICA-aided methodology to other blind MIMO equalization schemes.

ACKNOWLEDGEMENTS

V. Zarzoso is in receipt of a Post-doctoral Research Fellowship awarded by the Royal Academy of Engineering of the U.K.

REFERENCES

1. Ristaniemi T, Joutsensalo J. Advanced ICA-based receivers for block fading DS-CDMA channels. *Signal Processing* 2002; **82**(3):417–431.
2. Wireless World Research Forum. *7th Meeting*, Eindhoven, The Netherlands, December 3–4 2002.
3. Proakis JG. *Digital Communications* (4th edn). McGraw-Hill: New York, 2000.
4. Paulraj AJ, Papadias CB. Space–time processing for wireless communications. *IEEE Signal Processing Magazine* 1997; **14**(6):49–83.
5. van der Veen A-J, Talwar S, Paulraj A. A subspace approach to blind space–time signal processing for wireless communication systems. *IEEE Transactions on Signal Processing* 1997; **45**(1):173–190.
6. Tugnait JK, Tong L, Ding Z. Single-user channel estimation and equalization. *IEEE Signal Processing Magazine* 2000; **17**(3):16–28.
7. Sato Y. A method of self-recovering equalization for multi-level amplitude modulation. *IEEE Transactions on Communications* 1975; **23**:679–682.
8. Godard DN. Self-recovering equalization and carrier tracking in two-dimensional data communication systems. *IEEE Transactions on Communications* 1980; **28**(11):1867–1875.
9. Benveniste A, Goursat M, Ruget G. Robust identification of a nonminimum phase system: blind adjustment of a linear equalizer in data communications. *IEEE Transactions on Automatic Control* 1980; **25**:385–399.
10. Shalvi O, Weinstein E. New criteria for blind deconvolution of nonminimum phase systems (channels). *IEEE Transactions on Information Theory* 1990; **36**(2):312–321.
11. Shalvi O, Weinstein E. Super-exponential methods for blind deconvolution. *IEEE Transactions on Information Theory* 1993; **39**(2):504–519.
12. Tong L, Xu G, Kailath T. Blind identification and equalization based on second-order statistics: a time domain approach. *IEEE Transactions on Information Theory* 1994; **40**(2):340–349.
13. Moulines E, Duhamel P, Cardoso J-F, Mayrargue S. Subspace methods for the blind identification of multichannel FIR filters. *IEEE Transactions on Signal Processing* 1995; **43**(2):516–525.
14. Slock DTM. Blind fractionally-spaced equalization, perfect-reconstruction filter banks and multichannel linear prediction. In *Proceedings of the ICASSP-94, 19th International Conference on Acoustics, Speech and Signal Processing*, vol. IV. Adelaide, Australia, April 19–22, 1994; 585–588.
15. Mansour A. A mutually referenced blind multiuser separation of convolutive mixture algorithm. *Signal Processing* 2001; **81**(11):2253–2266.
16. Zarzoso V, Nandi AK, García JI, Domínguez LV. Blind identification and equalization of MIMO FIR channels based on second-order statistics and blind source separation. In *Proceedings of the DSP-2002, 14th International Conference on Digital Signal Processing*, vol. I. Santorini, Greece, July 1–3, 2002; 135–138.

17. Zarzoso V, Nandi AK, Igual-García J, Vergara-Domínguez L. Blind identification and equalization of MIMO FIR channels based on subspace decomposition and independent component analysis. In *Proceedings of the 2nd IMA International Conference on Mathematics in Communications*, University of Lancaster, UK, December 16–18, 2002.
18. Talwar S, Viberg M, Paulraj A. Blind separation of synchronous co-channel digital signals using an antenna array. Part I: Algorithms. *IEEE Transactions on Signal Processing* 1996; **44**(5):1184–1197.
19. van der Veen A-J, Paulraj A. An analytical constant modulus algorithm. *IEEE Transactions on Signal Processing* 1996; **44**(5):1136–1155.
20. van der Veen A-J. Analytical method for blind binary signal separation. *IEEE Transactions on Signal Processing* 1997; **45**(4):1078–1082.
21. Hyvärinen A, Karhunen J, Oja E. *Independent Component Analysis*. John Wiley & Sons: New York, 2001.
22. Cardoso J-F, Souloumiac A. Blind beamforming for non-Gaussian signals. *IEE Proceedings-F* 1993; **140**(6):362–370.
23. Comon P. Independent component analysis, a new concept? *Signal Processing* 1994; **36**(3):287–314.
24. Zarzoso V, Nandi AK. Exploiting non-Gaussianity in blind identification and equalization of MIMO FIR channels. *IEE Proceedings—Vision, Image and Signal Processing* (*Special Issue on Nonlinear and non-Gaussian Signal Processing*) 2004;**151**(1):69–75.
25. Xu G, Liu H, Tong L, Kailath T. A least-squares approach to blind channel identification. *IEEE Transactions on Signal Processing* 1995; **43**(12):2982–2993.
26. Gesbert D, Duhamel P, Mayrargue S. On-line blind multichannel equalization based on mutually referenced filters. *IEEE Transactions on Signal Processing* 1997; **45**(9):2307–2317.
27. Giannakis GB, Halford SD. Blind fractionally spaced equalization of noisy FIR channels: direct and adaptive solutions. *IEEE Transactions on Signal Processing* 1997; **45**(9):2277–2291.
28. Shen J, Ding Z. Direct blind MMSE channel equalization based on second-order statistics. *IEEE Transactions on Signal Processing* 2000; **48**(4):1015–1022.
29. Gesbert D, Duhamel P, Mayrargue S. Blind multichannel adaptive MMSE equalization with controlled delay. In *Proceedings of the SSAP-1996, IEEE Statistical Signal and Array Processing Workshop*, Corfu, Greece, June 24–26, 1996; 172–175.
30. Gazzah H, Abed-Meraim K. Blind ZF equalization with controlled delay robust to order over estimation. *Signal Processing* 2003; **83**(7):1505–1518.
31. Prandini M, Campi MC, Leonardi R. Optimal delay estimation and performance evaluation in blind equalization. *International Journal of Adaptive Control and Signal Processing* 1997; **11**(7):621–640.
32. Zarzoso V. Exploiting independence for co-channel interference cancellation and symbol detection in multiuser digital communications. In *Proceedings of the ISSPA-2003, 7th International Symposium on Signal Processing and its Applications*, Paris, France, July 1–4, 2003.
33. Abed-Meraim K, Loubaton P, Moulines E. A subspace algorithm for certain blind identification problems. *IEEE Transactions on Information Theory* 1997; **43**(2):499–511.
34. Yang HH. On-line blind equalization via on-line blind separation. *Signal Processing* 1998; **68**(3):271–281.
35. Zhang Y, Kassam SA. Blind separation and equalization using fractional sampling of digital communications signals. *Signal Processing* 2001; **81**(12):2591–2608.
36. Hyvärinen A, Oja E. A fast fixed-point algorithm for independent component analysis. *Neural Computation* 1997; **9**(7):1483–1492.

